

# Influence of the microstructure on the macroscopic elastic and optical properties of dried sonogels: A Brillouin spectroscopic study

R. J. Jiménez-Riobóo,<sup>a)</sup> M. García-Hernández,<sup>b)</sup> and C. Prieto  
*Instituto de Ciencia de Materiales de Madrid, C.S.I.C., Cantoblanco, E-28049-Madrid, Spain*

J. J. Fuentes-Gallego, E. Blanco, and M. Ramírez-del-Solar  
*Departamento de Física de la Materia Condensada, Universidad de Cádiz, Apartado 40, 11510-Puerto Real, Cádiz, Spain*

Received 9 December 1996; accepted for publication 24 February 1997)

The elastic and optical properties of organically modified silicates prepared by ultrasonics aided polycondensation of tetraethoxysilane and polydimethylsiloxane are studied by means of high resolution Brillouin spectroscopy. Nuclear magnetic resonance data evidence the microseparation of the organic and inorganic phases for the systems with high content of polymer formation. The elastic and optical properties are clearly influenced by the change in microstructure. We propose a three component mechanical model that qualitatively explains the observed variation of the elastic constant  $c_{11}$  versus molar fraction of dimethylsiloxane in these vitreous materials and develop a structural model that accounts for the observed dynamical behavior. © 1997 American Institute of Physics. [S0021-8979(97)04911-6]

## I. INTRODUCTION

The unique properties of organically modified silicates (ORMOSIL) as produced by the sol-gel methods have recently made the study of these materials a fast growing field.<sup>1,2</sup> In particular, the macroscopic elastic properties of rubberlike materials obtained by hydrolysis and ulterior polycondensation of organic polymers with inorganic silica based precursors have been fully explored by standard methods (basically Young's Modulus measurements) since the early work by Mackenzie *et al.*<sup>3</sup> However, little attention has been paid to the dynamical elastic behavior of these materials and its correlation to the macroscopically observed properties. This is a major point since a full understanding of the interplay between structural and dynamical correlations is required so as to tailor the mechanical properties of these novel materials. Within this frame the knowledge of the different possible conformations in ORMOSILs resulting from differences in the chemical bonding between the inorganic precursor and the organic component seems to be essential. According to nuclear magnetic resonance (NMR) data,<sup>4</sup> at the lowest concentrations of the organic compound polydimethylsiloxane (PDMS) in the sample, the probability of bonding between the inorganic component and the organic material in sites different from the two extrema of the organic chain is very high, while competing processes of autocondensation for the organic component are minimized. Therefore a more efficient interbonding of the inorganic and organic components occurs.<sup>5</sup> However, microphase separation has been observed for related systems using a great variety of techniques probing either dynamical or structural aspects of these materials.<sup>4-6</sup>

As a model material we have studied a series of ORMOSILs obtained from chemical combination of tetra-

ethoxysilane (TEOS) and PDMS with different concentration ratios. The investigated set of samples were prepared by the sol-gel route, following the sonogel procedure.<sup>7,8</sup>

In order to obtain a clear understanding of the relationship between the structure and the elastic properties (static and dynamical) of ORMOSILs, we have made use of high performance Brillouin spectroscopy on these materials. Brillouin scattering has proven to be an essential technique to disentangle the fundamental aspects of the viscoelastic and elastic properties of a broad range of amorphous materials,<sup>9</sup> while also providing important information on the optical properties of the samples explored. Parallel to the Brillouin measurements we have performed NMR experiments on ORMOSIL samples with different concentrations of the organic component. The combined analysis of the experimental results obtained by both techniques renders a very interesting picture of the micromorphology of sono-ORMOSILs and its influence on the macroscopic mechanical properties.

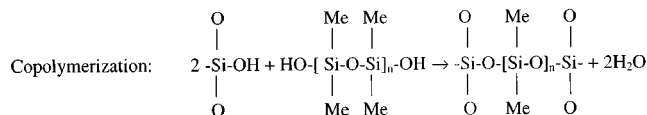
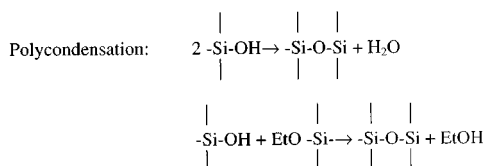
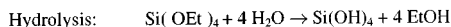
## II. EXPERIMENT

### A. Sample preparation and characterization

TEOS from Merck ( $n=1.38$ ,  $\rho=0.983 \text{ g cm}^{-3}$ ) was used as an inorganic precursor and PDMS, with an average molecular weight of 550, from Hüls America Inc. ( $n=1.40$ ,  $\rho=0.950 \text{ g cm}^{-3}$ ), as an organic component. This PDMS has been chosen as an organic precursor based on its appropriated density and steric hindrance due to the methyl group. HCl acid was utilized as a catalyst. In order to avoid the use of additional organic solvents that decrease the gels density, a high powered ultrasound probe (20 kHz, 15 W) has been employed. The reactions taking place in the synthesis of ORMOSILs are:

<sup>a)</sup>Electronic mail: rafa@cc.csic.es

<sup>b)</sup>On leave from Instituto de Estructura de la Materia, C.S.I.C.



HCl acid and ultrasound energy mainly promote the hydrolysis reaction giving rise to gels of higher density formed by smaller particles than those processed by the classic method. When the organic network precursor, PDMS, is added to the TEOS/H<sub>2</sub>O/HCl system, the copolymerization reaction described above takes place, competing with the silic acid self-condensation and other possible reactions. In fact, the high reactivity of PDMS can induce its self-polymerization, leading to fully organic linear or cyclic structure. In the latter case, there is a phase separation between the organic and inorganic networks. Thus, the processing method followed tried to minimize this unwanted reaction and avoid phase separation resulting from differences between TEOS and PDMS reactivity. In the first step, TEOS is prehydrolyzed by subjecting a mixture of TEOS: acidic water (1:2 molar ratio) to the ultrasound radiation dose  $E_s = 60 \text{ J cm}^{-3}$ . Then adequate amounts of PDMS, ranging from 0 to 40 wt % referred to TEOS, was added and an additional ultrasonic energy was applied to complete the total energy dose of  $0.12 \text{ kJ cm}^{-3}$ . The resulting solution gels after a period of time varying from 30 min to 1 week when increasing PDMS content. Finally, samples were aged in closed containers for 1 week and dried for at least 2 weeks with a holed parafilm on the top of the opened vessel. The resulting monolithic samples of ORMOSILs are transparent for the lower doses of the organic component but become milky for the higher one, probably due to the inorganic phase inability to incorporate homogeneously a great amount of the organic phase, at least for this method.

For the sake of clarity the organic fraction in the hybrid material will be expressed in the following as monomer molar fraction, that is, DMS mol/(TEOS mol + DMS mol)%. Sample volume was measured with two different probes in order to estimate the ORMOSILs densities at two different resolution levels. Bulk densities were evaluated by the Archimedes method using cyclohexane ( $\rho = 0.78 \text{ g cm}^{-3}$ ). The density of the hybrid organic-inorganic skeleton was estimated from helium pycnometry in a noncommercial vacuum line.

In order to obtain filmlike samples of ORMOSILs we deposited part of the obtained sol in a silicone rubber cell. The silicone rubber allows the films to be easily removed without any strain after gelification in the cell. In this way we obtained free standing films of about  $10 \mu\text{m}$  thickness with plane parallel faces suitable for use in Brillouin spectroscopic experiments.

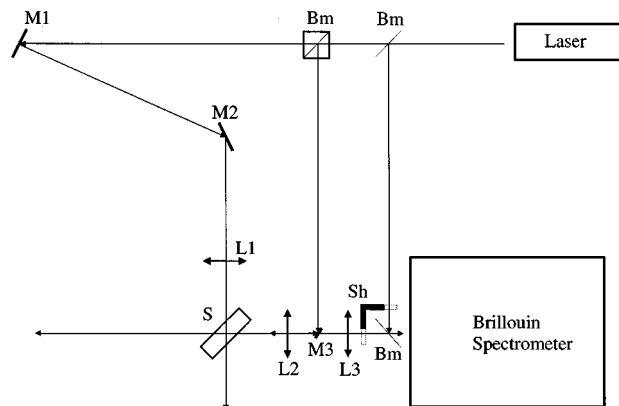


FIG. 1. Experimental setup used to perform the Brillouin scattering experiments: Bm: beam splitter, M1..3: optical mirrors, L1..3: optical lenses, Sh: light shutter, S: sample.

## B. Brillouin spectroscopy

The Brillouin spectrometer used is based on a 3+3-Pass Fabry-Perot interferometer in tandem<sup>10</sup> with an Ar-ion single mode laser as the light source. The experimental setup is schematically drawn in Fig. 1. This setup allows the simultaneous realization of the backscattering ( $180^\circ$ ) geometry and the special  $90^\circ$  scattering geometry (for the  $90^\circ$  configuration we will use the 90A notation following that used in the literature).<sup>11-13</sup> The principles of the 90A and backscattering ( $180^\circ$ ) geometries are shown in Fig. 2. In monolithic samples we have recorded separately the 90A and the backscattering spectra. In the case of filmlike samples of a few  $\mu\text{m}$  thickness the experimental configuration for the 90A scattering geometry gives rise simultaneously to a supplementary backscattering due to the different refractive indices between the surrounding air and the sample.<sup>13</sup> The corresponding phonon wavelengths are:

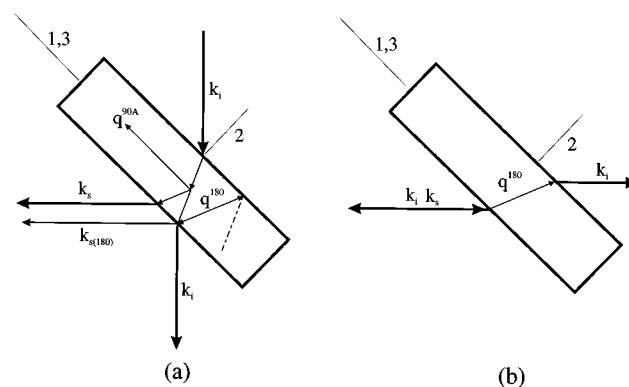


FIG. 2. Schematic drawing of the principles of the (a) 90A and (b) backscattering ( $180^\circ$ ) geometries.  $k_{i,s}$  represent the incident and scattered light wave vectors respectively;  $q$  represents the phonon wave vector involved. Reflection in the interface sample-air gives rise to a supplementary backscattering ( $180^\circ$ ) process in the 90A scattering geometry conformation (a).

$$\Lambda^{90A} = \frac{\lambda_0}{\sqrt{2}}; \quad \Lambda^{180} = \frac{\lambda_0}{2n_i}, \quad (1)$$

where  $\lambda_0$  is the laser wavelength in vacuum (514.5 nm in our case) and  $n_i$  is the relevant refractive index of the sample. In the case of an isotropic sample there exists only one refractive index and the phonon wave vectors are symmetry equivalent. As it has been discussed elsewhere, in the case of the 90A scattering geometry, the influence of the birefringence on the acoustic wavelength can be omitted.<sup>13</sup> Depending on the scattering geometry the sound velocity is related to the Brillouin line shift,  $f$  (in frequency), as follows:

$$v^{90A} = f^{90A} \frac{\lambda_0}{\sqrt{2}}; \quad v^{180} = f^{180} \frac{\lambda_0}{2n_i}. \quad (2)$$

Notice that in the case of no acoustic dispersion these velocities must be strictly the same. Taking advantage of this fact it is straightforward to obtain a relation between the Brillouin frequency and the refractive index of the sample under study in the following way:

$$n_i = \frac{f^{180}}{f^{90A} \sqrt{2}}. \quad (3)$$

This is a very particular case of the more general  $D$  function defined in Ref. 9.

The stiffness coefficient,  $c$ , related to the measured sound velocity obeys the relation  $c = \rho v^2$  where  $\rho$  is the mass density of the material. In an acoustic isotropic system there exist only two independent elastic constants: The longitudinal one,  $c_{11}$ , and the shear (transverse) one,  $c_{44}$ . Depending on the polarization conditions of the incident and scattered light it is possible to select one of them.<sup>14</sup>

In order to evaluate the elastic constant  $c_{11}$ , we used density values stemming from He picnometry given by  $\rho(\text{g/cm}^3) = 1.726 - 0.00945 \times M$  ( $M$  being the molar fraction of DMS). We could also obtain density values for samples containing 0% and 41.6% molar fraction of DMS using  $\text{C}_6\text{H}_{12}$  picnometry. In the case of the 0% sample both picnometries give the same density value while in the case of the 41.6% sample the  $\text{C}_6\text{H}_{12}$  picnometry gives a 15% lower value. This fact indicates a clear decrease in pore size with the inclusion of PDMS.

### C. NMR

High resolution  $^{29}\text{Si}$  magic angle spinning (MAS) and cyclic polarization magic angle spinning (CPMAS) NMR spectra of powdered samples were recorded at 79.49 MHz, by spinning at the magic angle  $50^\circ 44'$ . The experiments were performed on spectrometer Bruker MSL 400 equipped with a Fourier transform unit. The spinning frequency was 4000 cps and the applied magnetic field is 9.4 T.  $^{29}\text{Si}$  MAS spectra were collected with the single pulse program CYCLOPS using a pulse width of 6  $\mu\text{s}$  (90 A) and 10 s recycle delay. All measurements were conducted at room temperature using tetramethylsiloxane as external standard reference and accumulations amounted to 400 free induction decays (FIDs).

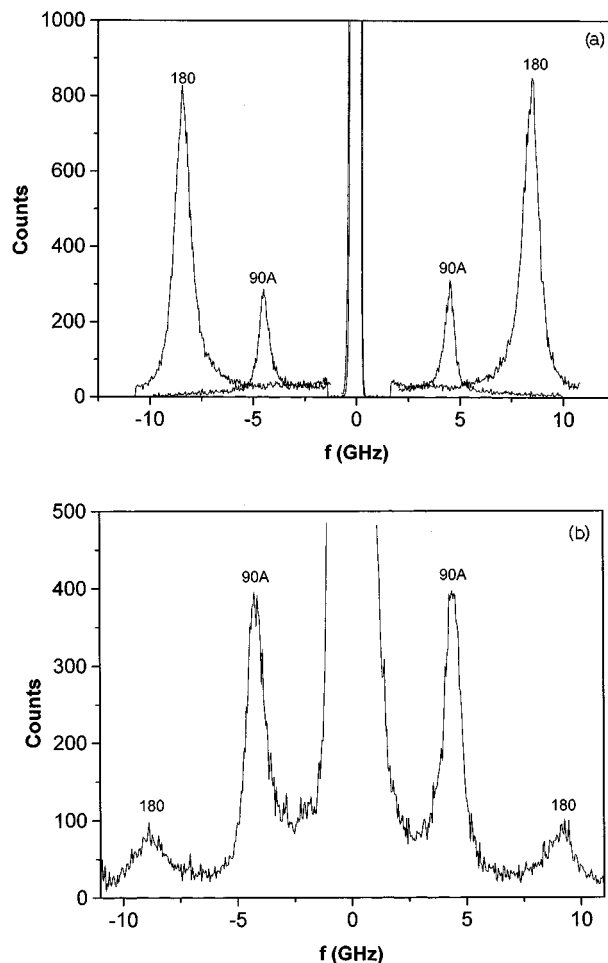


FIG. 3. Typical recorded spectra in the case of (a) a monolithic sample and of (b) a filmlike sample. In (a) the 90A and the backscattering ( $180^\circ$ ) spectra are plotted simultaneously. In the case of the filmlike sample (b) the spectrum recorded in the 90A scattering geometry clearly shows the supplementary backscattering contribution ( $180^\circ$ ).

### III. RESULTS AND DISCUSSION

Typical spectra in the case of a monolithic sample and of a filmlike sample are shown in Figs. 3(a) and 3(b). A Lorentzian function was used in order to obtain the frequency and the half width at half maximum (HWHM) from the Brillouin peaks. We obtained a reliable estimation of the hypersonic attenuation by subtracting the HWHM of the Rayleigh line (central line) from the HWHM of the Brillouin peaks. From the optical and elastic point of view sonogels can be considered isotropic and therefore the elastic and optical indicatrices show only one value for the refractive index ( $n$ ) and for the longitudinal ( $c_{11}$ ) and the shear ( $c_{44}$ ) elastic constants. We were not able to obtain information about the shear elastic constant. This fact may be due to a severe overdamping of the shear acoustic modes in these porous materials. Moreover the presence of any broad central mode was not detected and the presence of fast relaxations in the explored systems cannot be inferred. As a result of the small thickness of the sample, the difference in refractive index with the surrounding air and the finite size of the scattering volume, it has been possible, using only the 90A scattering geometry

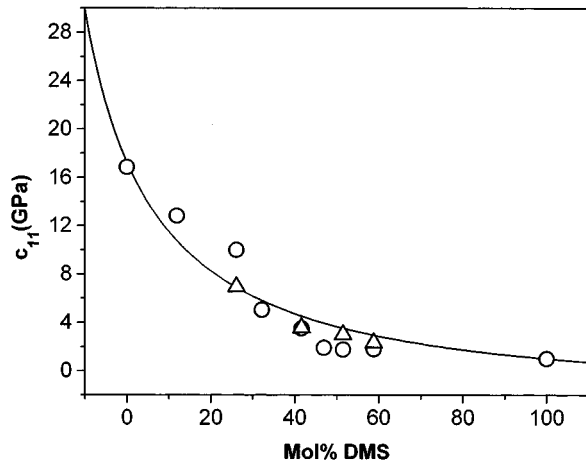


FIG. 4. DMS concentration dependence of the longitudinal elastic constant  $c_{11}$  for the monolithic samples ( $\circ$ ) and for the filmlike samples ( $\Delta$ ). The full line represents the best fit of the experimental data to Eq. (4).

(see Sec. II B and Fig. 2), to obtain in the same spectrum and simultaneously, information about the 90A and the backscattering processes [Fig. 3(b)].

The influence of the DMS concentration in the static and dynamical elastic properties of sonogels is clearly demonstrated in Figs. 4 and 5. It is very interesting to notice that the preparation conditions of the samples (monolithic or filmlike) does not influence the values of the  $c_{11}$  elastic constant (Fig. 4).

As far as we do not know the phonon wave vector dependence of the hypersonic attenuation,  $\Gamma$ , (HWHM) it is only possible to perform a qualitative comparison between the 90A (filmlike samples) and backscattering (monolithic samples) attenuation data. Figures 5(a) and 5(b) show a very similar DMS concentration behavior of  $\Gamma$  in both cases.  $\Gamma$  diminishes with increasing PDMS content, shows a minimum of about 40%, and increases for higher DMS concentration values. This fact indicates that the backscattering technique in monolithic samples gives reliable results despite the milky aspect of the samples with the highest concentration. The thin samples (about 10  $\mu\text{m}$ ) are not affected by the transparency problems of the monolithic ones.

The concentration behavior of  $c_{11}$  is different from that of  $\Gamma$ . There is a smooth softening of the elastic constant with increasing DMS concentration, tending asymptotically to the value of the pure PDMS, with no relevant anomaly at a defined PDMS content. The asymptotic behavior is reached at concentration values about 40% of DMS. Previous results concerning the DMS concentration dependence of  $c_{11}$  and  $\Gamma$  are confirmed by these more complete measurements.<sup>15</sup>

The usual experiments to determine the mechanical properties of dried ORMOSILs have been interpreted in terms of the interconnection of two different elastic media (either as a series connection or as a parallel connection), one being the  $\text{SiO}_2$  matrix and the other one the incorporated polymer (in our case PDMS).<sup>3</sup> The proposed models give no satisfactory explanation of the elastic behavior. The Brillouin spectroscopy offers new information concerning the hypersonic attenuation,  $\Gamma$ . This attenuation is related to the inverse

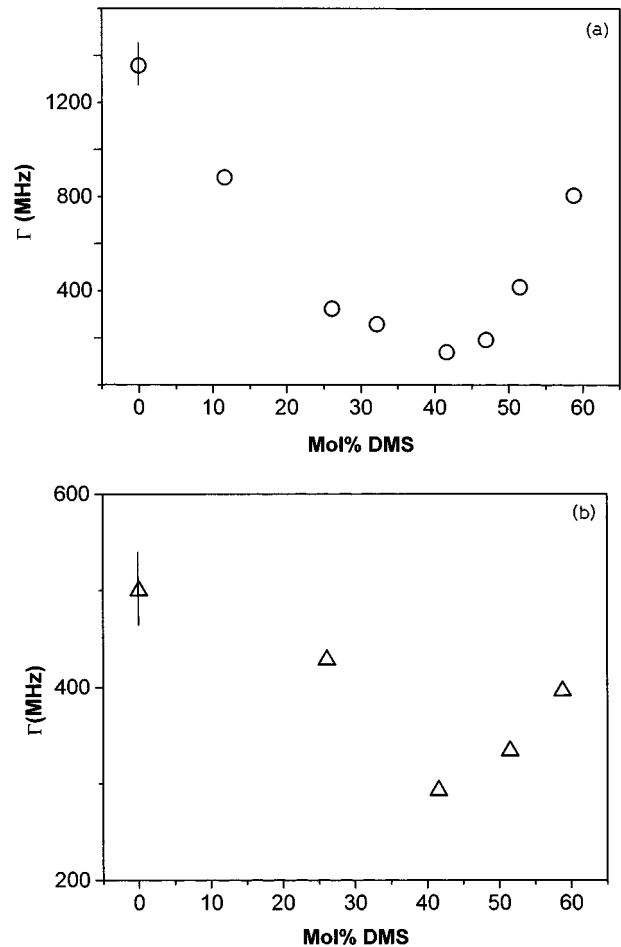


FIG. 5. DMS concentration dependence of the hypersonic attenuation ( $\Gamma$ ): (a) backscattering geometry (monolithic samples), (b) 90A scattering geometry (filmlike samples). The straight line on the first experimental point gives the experimental error in the estimation of the attenuation in both cases.

of the phonon lifetime,  $\tau$ , ( $\Gamma=1/\tau$ ), and must be taken into account to propose a morphological model to explain the elastic behavior. Interpreting the attenuation in terms of phonon lifetimes it is possible to explain the attenuation behavior in terms of changing number of interphases in the material (i.e., porosity and microsegregation). A physical picture of the system emerges in which two plausible PDMS forms in the sample (segmentlike and globular) co-exist. For low concentration of PDMS the inclusion of organic material in the silica network takes place quite uniformly as chains embedded in the silica matrix. The enrichment in PDMS together with the decrease in porosity of the material are reflected by a decay in the hypersonic attenuation. However, a lower pore density would imply an increase in the elastic constant which is not observed.<sup>16</sup> Therefore, the measured decay (Fig. 4) can only be explained by a renormalization of the elastic properties of the gel due to the linking of PDMS to TEOS. This situation remains until the PDMS concentration is high enough to allow the globular configuration of PDMS to preferentially establish. This is consistent with the fact that at high polymer concentrations the globular form is, from the thermodynamic point of view, more stable.<sup>17</sup> A side

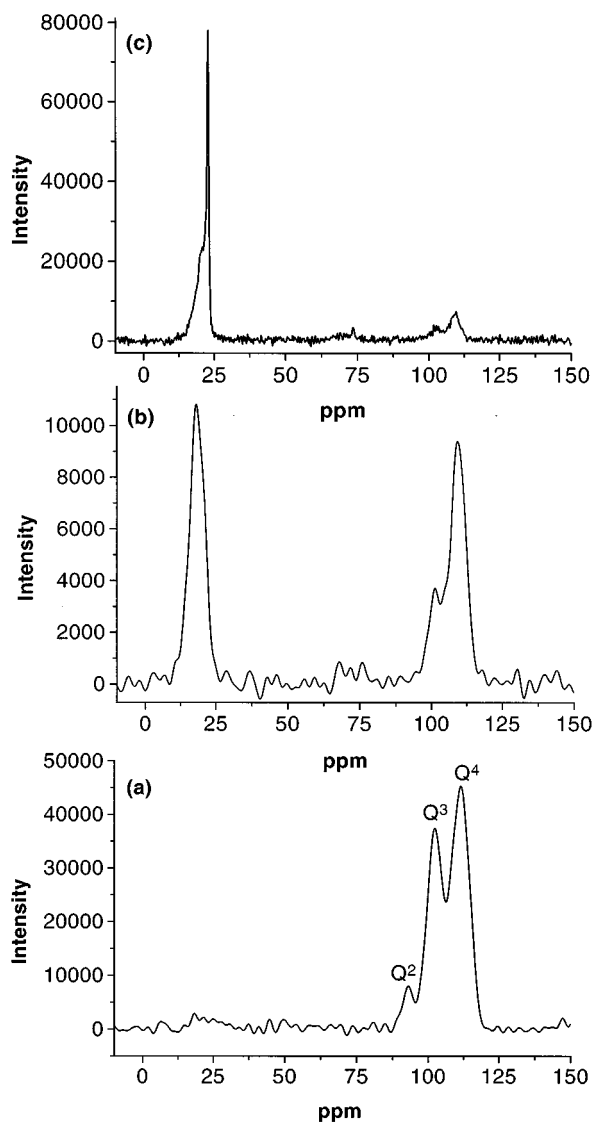


FIG. 6.  $^{29}\text{Si}$  NMR spectra of ORMOSIL powder samples of different DMS concentrations: (a) 0%, (b) 41.6%, (c) 58.8%.  $Q^2$ ,  $Q^3$ , and  $Q^4$  represent different silicon nuclei after Ref. 18.

product of this structural change towards some sort of microphase separation is the building up of liquidlike islands and, consequently, the lifetime of the phonons decreases while some sort of “saturated” value is reached for the elastic constant  $c_{11}$ . The difference in the observed linewidths at these high PDMS concentrations in relation to the measured linewidth for liquid PDMS (0.7 GHz in backscattering) can be understood in terms of the porosity of the gels and severe changes in the acoustic impedances when the phonon crosses the interphase limiting the liquid islands.

Within this scenario any model intending to describe the static elastic properties should take into account the existence of the PDMS in two different morphologies (segment-like and globular) and not only one (segmentlike) as has been done until now. In order to test our working hypothesis on the coexistence of two PDMS forms we have conducted a series of  $^{29}\text{Si}$  NMR experiments on the same sample set. Figure 6 shows the NMR spectra corresponding to the 0,

41.6, and 58.8 mol % DMS for an easy comparison. As can be seen in Fig. 6(a) the spectrum corresponding to the pure TEOS compound shows the typical three peaked feature of a well structured silica backbone gel. We have fit the data in terms of three Gaussians, corresponding to three different environments of the  $^{29}\text{Si}$  nucleus in vitreous silica gels, centered at 111.30, 102.078, and 92.74 ppm being respectively assigned to silicon nucleus of type  $Q^4$ ,  $Q^3$ , and  $Q^2$ , according to the standard notation.<sup>18</sup> This structuration of the silica network can be understood in terms of quasispherical clusters conforming the pure TEOS compound.<sup>19</sup> These clusters contain a hard core formed by silicon nuclei bonded to four oxygens (type  $Q^4$ ) and surrounded by other silicon nuclei bonded to three or two oxygens (type  $Q^3$  and  $Q^2$ , respectively), the latter connecting the core with the pores of the system.

Following the model proposed in Ref. 19, the ratio of the integrated intensities of the fitted Gaussians renders an estimate of the mean cluster radius, being in this case of the order of 15 Å. Figure 6(b) shows the spectrum of the sample containing 41.6% DMS. Apart from the peaks corresponding to silicon nuclei in a silica network, not as well defined as in the previous case, a new asymmetric peak appears in the low ppm range stemming from silicon nuclei inserted in PDMS segments. The intensity in this region can be accounted for by two Gaussians centered at 17.7 and 21.1 ppm being the first one order of magnitude more intense than the second. Following the assignments made by Mackenzie in similar systems,<sup>4,7</sup> these two components can be assigned respectively to  $(-\text{O}-)_3\text{Si}-\text{O}-\text{Si}^*(\text{CH}_3)_2-\text{O}-\text{Si}=\text{}$  and  $-\text{Si}(\text{CH}_3)_2-\text{O}-\text{Si}^*(\text{CH}_3)_2-\text{O}-\text{Si}(\text{CH}_3)_2-$ . From the intensity ratio of these two components it seems clear that the intimate mixture of TEOS and PDMS has proceeded almost in a complete way. Figure 6(c) shows the corresponding spectrum for the 58.8% DMS sample. The most dramatic change in the spectrum regarding Fig. 6(b) is the appearance of an extremely narrow component (resolution limited) centered at 22.7 ppm and a strong decrease of intensity in the [16–18 ppm] region. The narrow peak closely resembles those found for liquid PDMS in real time NMR experiments just after mixing the organic and inorganic components prior to any reaction scheme.<sup>4,7</sup> This fact confirms our hypothesis of the existence of liquidlike islands of PDMS in a quasispherical form for gels with a high content of PDMS (51.5%–58.8%). It is equally remarkable concerning the decrease of any intensity around 17 ppm implying a decrease of chemical connection between the organic and the inorganic components of our sonogels.

The interpretation of the elastic data in terms of two coexisting morphologies of PDMS has been clearly supported by the NMR results. It is therefore necessary to include these different forms of PDMS in the models describing the static elastic properties. Following the lines of the two extreme models proposed by Mackenzie,<sup>3</sup> we propose a mathematical model that qualitatively explains the observed elastic behavior. The main ingredient of our model is the consideration of two morphologically different forms of PDMS whose relative contributions to the observed elastic behavior are normalized to the total content of PDMS in the

TABLE I. Values obtained from a least square's fit of Eq. (4) to the experimental data.

$c_1$ (GPa)	$c_2$ (GPa)	$c_3$ (GPa)
$17 \pm 2$	$3 \pm 1$	1.018

sample. Both forms, PDMS in a segmentlike configuration within the backbone of the  $-\text{SiO}_2-$  network and PDMS in a quasiglobular (liquidlike) configuration, are parallel branched while being branched in series to the  $-\text{SiO}_2-$  structure. The model reads

$$c_{11} = \frac{1}{\left( \frac{1-x}{c_1} + \frac{x}{c_2(1-x) + c_3x} \right)}, \quad (4)$$

where  $x$  is the molar fraction of DMS monomer,  $c_1$  refers to the elastic constant of silica,  $c_2$  and  $c_3$  are the elastic constants of PDMS in a segmentlike and globularlike configuration, respectively. The fitted parameters in our model are  $c_1$  and  $c_2$ ;  $c_3$  being constrained to the value of the elastic constant of liquid PDMS. This assumption is physically sound since no solid form of the polymer can be softer than the corresponding liquid and, in fact, none of the measured values for  $c_{11}$  lies below this limit. As it can be seen in Fig. 4 the model, in spite of its simplicity, describes the elastic behavior of the sonogels on semi-quantitative grounds. The values of the best fit for the fitting parameters are shown in Table I.

Despite the simplicity of the model, the obtained values for the elastic constants of the ORMOSILs are physically relevant.  $c_1$  is very similar to the measured value for the porous silica (0%) and  $c_2 > c_3$  reflects the well known fact that the elastic constant along the extended carbon chain is much higher than the one in a direction perpendicular to the carbon chain as in the case of  $n$ -alkanes<sup>20</sup> or semi-crystalline polymers.<sup>21</sup>

Since Brillouin spectroscopy is an optical technique we can also obtain, simultaneously to the elastic properties, information about the optical properties of the investigated samples. Combining the 90A and the backscattering geometries as in the case of the filmlike samples, it is possible to obtain an estimation of the refractive index at room temperature and for  $\lambda=514.5$  nm. One must remember that this is only possible because we are dealing with optically isotropic samples and that the related phonon wave vectors are symmetry equivalent (see Sec. II A). To our knowledge this is the first time that such a determination of the refractive index in these kinds of samples and for high PDMS content has been made. It is important to remember that for high PDMS content the monolithic samples present some milky aspect (optical dispersion)<sup>15</sup> and therefore it is not possible to obtain reliable values for the refractive index by means of conventional techniques. Following Eq. (3) it is easy to obtain an estimation of the refractive index  $n_{514.5}^{\text{RT}}$  only from the position of the Brillouin peaks. Figure 7 shows the DMS-concentration dependence of  $n_{514.5}^{\text{RT}}$ . As it is shown in Fig. 7 and in contrast to the elastic behavior (static and dynamical),

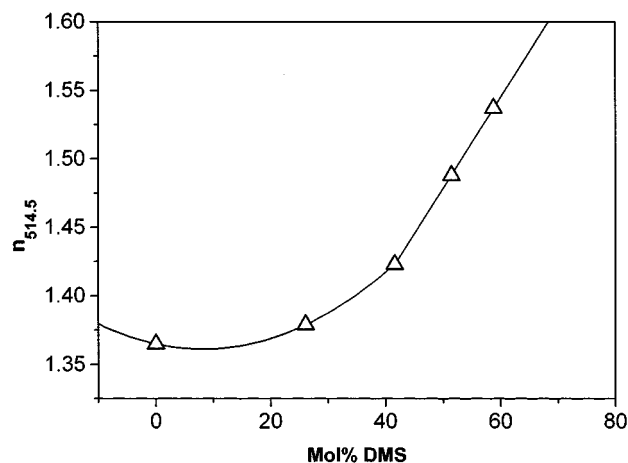


FIG. 7. DMS concentration behavior of the refractive index  $n_{514.5}^{\text{RT}}$ . The full line is only a guide to the eye.

the refractive index is a slow varying function of DMS content in the sample up to concentrations around 26 mol % of DMS. For higher PDMS content, above 40 mol %,  $n_{514.5}^{\text{RT}}$  increases monotonically following a linear dependence. The guide line in Fig. 7 suggests the existence of a minimum in  $n_{514.5}^{\text{RT}}$  but one has to be very careful so as not to overinterpret the results. The refractive index shows a clear crossover between two different regimes at a DMS concentration of about 40 mol %. Similar to the elastic properties, the optical properties also reflect the appearance of microsegregation in these samples.

#### IV. CONCLUSIONS

Monolithic and filmlike (few  $\mu\text{m}$  thickness) ORMOSIL samples have been the object of this study by means of NMR and Brillouin spectroscopy. High resolution Brillouin spectroscopy has proven to be an ideal technique to study not only the elastic properties of ORMOSILs but also to obtain very valuable information about the optical properties. The elastic properties are not affected by the filmlike or monolithic nature of the samples. From the measured dynamic and static hypersonic properties, the elastic constant  $c_{11}$ , and the related hypersonic attenuation  $\Gamma$ , can be extracted. The combined interpretation of the NMR data and the elastic properties gives rise to a structural model that takes into account the existence of microsegregation of the ORMOSIL components above a defined DMS concentration. This microsegregation manifests itself in the existence of two different conformations of the PDMS component (segmentlike and globular), the first inserted within the backbone of the  $-\text{SiO}_2-$  network and the second forming liquidlike islands. The proposed static elastic model to interpret the DMS concentration dependence of the elastic constant  $c_{11}$ , takes into account the existence of these two different PDMS conformations and despite its simplicity, describes the elastic behavior of the sonogels on semi-quantitative grounds. For the first time also the optical properties of the ORMOSILs have been estimated. The refractive index,  $n_{514.5}^{\text{RT}}$ , of the studied samples is also sensitive to the existence of a characteristic DMS concentration.

## ACKNOWLEDGMENTS

The authors want to thank Professor Dr. J. Sanz and Dr. L. Sobrados for the assistance with the NMR experiments. Special thanks go to Professor Dr. J. K. Krüger of the Saarbrücken University for illuminating discussions. This work has been partially supported by Junta de Andalucía (Exp No. 6015) and by CICYT (Proj. Nos. MAT-95-0040-C02-02 and MAT-94-722).

- <sup>1</sup>J. D. Mackenzie, Y. J. Chung, and Y. Hu, *J. Non-Cryst. Solids* **147&148**, 271 (1992).
- <sup>2</sup>Y. Hoshino and J. D. Mackenzie, *J. Sol-Gel Sci. Technol.* **5**, 83 (1996).
- <sup>3</sup>Y. Hu and J. D. Mackenzie, *J. Mater. Sci.* **27**, 4415 (1992) and references therein.
- <sup>4</sup>T. Iwamoto, K. Morita, and J. Mackenzie, *J. Non-Cryst. Solids* **159**, 65 (1993).
- <sup>5</sup>H. Huang, B. Orlor, and G. L. Wilkes, *Macromolecules* **20**, 1322 (1987).
- <sup>6</sup>N. Micali, C. Vasi, F. Mallamace, R. Bansil, S. Pajevic, and F. Sciortino, *Phys. Rev. E* **48**, 4501 (1993).
- <sup>7</sup>T. Iwamoto and J. D. Mackenzie, *J. Sol-Gel Sci. Technol.* **4**, 141 (1995).
- <sup>8</sup>L. Esquivias and J. Zarzycki, in *Ultrastructure Processing of Advanced Ceramics*, edited by J. D. Mackenzie and D. R. Ulrich (Wiley, New York, 1987), p. 255.
- <sup>9</sup>J. Kruger, in *Optical Techniques to Characterize Polymer Systems*, edited by H. Bassler (Elsevier, Amsterdam, 1989), p. 429.
- <sup>10</sup>J. R. Sandercock, "Trends in Brillouin Scattering," in *Topics in Applied Physics* (Springer, Berlin, 1982), Vol. 51, p. 173.
- <sup>11</sup>J. K. Krüger, L. Peetz, and M. Pietralla, *Polymer* **19**, 1397 (1978).
- <sup>12</sup>J. K. Krüger, M. Pietralla, and H.-G. Unruh, *Col. Pol. Sci.* **261**, 409 (1983); *Phys. Status Solidi A* **71**, 493 (1982).
- <sup>13</sup>J. K. Krüger, A. Marx, L. Peetz, R. Roberts, and U. G. Unruh, *Col. Pol. Sci.* **264**, 403 (1986).
- <sup>14</sup>B. A. Auld, *Acoustic Fields and Waves in Solids* (Wiley, New York, 1973).
- <sup>15</sup>M. García-Hernández, R. J. Jiménez-Riobóo, C. Prieto, J. J. Fuentes-Gallego, E. Blanco, and M. Ramírez-del-Solar, *Appl. Phys. Lett.* **69**, 3827 (1996).
- <sup>16</sup>R. M. Christiansen, *Mechanics of Composite Materials* (Krieger, Malabar, FL, 1991).
- <sup>17</sup>P. J. Flory, *Principles of Polymer Chemistry* (Cornell University Press, Ithaca, New York, 1953), Chapter X.
- <sup>18</sup>G. Engelhardt and D. Michel, *High-Resolution Solid-State NMR of Silicates and Zeolites* (Wiley, New York, 1987).
- <sup>19</sup>M. J. Muñoz, M. Gregorkiewltz, and F. J. Bermejo, *J. Non-Cryst. Solids* **189**, 90 (1995).
- <sup>20</sup>R. Jiménez, J. K. Krüger, K.-P. Bohn, and C. Fischer, *J. Phys., Condens. Matter.* **8**, 757 (1996).
- <sup>21</sup>J. K. Krüger, B. Heydt, C. Fischer, J. Baller, R. Jiménez, K.-P. Bohn, B. Servet, P. Galtier, M. Pavel, B. Ploss, M. Beghi, and C. Bottani, *Phys. Rev. B* **55**, 3487 (1997).